J Antimicrob Chemother 2021; **76**: 1703–1711
doi:10.1093/jac/dkab106 Advance Access publication 5 April 2021

Journal of Antimicrobial Chemotherapy

Evolution and genomic insight into methicillin-resistant *Staphylococcus aureus* ST9 in China

Nansong Jiang[1], Kelly L. Wyres [2], Jun Li[1,3], Andrea T. Feßler[4], Henrike Krüger[4], Yang Wang[1], Kathryn E. Holt[2,5], Stefan Schwarz [1,4] and Congming Wu[1]*

[1]*Beijing Key Laboratory of Detection Technology for Animal Food Safety, College of Veterinary Medicine, China Agricultural University, Beijing, China;* [2]*Department of Infectious Diseases, Central Clinical School, Monash University, Melbourne, Victoria 3004, Australia;* [3]*Institute of Medicinal Biotechnology, Chinese Academy of Medical Sciences, Beijing, China;* [4]*Institute of Microbiology and Epizootics, Centre for Infection Medicine, Department of Veterinary Medicine, Freie Universität Berlin, Berlin, Germany;* [5]*Department of Infection Biology, London School of Hygiene & Tropical Medicine, London, UK*

*Corresponding author. E-mail: wucm@cau.edu.cn

Received 15 October 2020; accepted 13 March 2021

Objectives: To reconstruct the evolutionary history and genomic epidemiology of *Staphylococcus aureus* ST9 in China.

Methods: Using WGS analysis, we described the phylogeny of 131 *S. aureus* ST9 isolates collected between 2002 and 2016 from 11 provinces in China, including six clinical samples from Taiwan. We also investigated the complex structure and distribution of the *lsa*(E)-carrying multiresistance gene cluster, and genotyped prophages in the genomes of the ST9 isolates.

Results: ST9 was subdivided into one major ($n = 122$) and one minor ($n = 9$) clade. Bayesian phylogeny predicted the divergence of ST9 isolates in pig farming in China as early as 1987, which then evolved rapidly in the following three decades. ST9 isolates shared similar multiresistance properties, which were likely acquired before the ST9 emergence in China. The accessory genome is highly conserved, and ST9 harboured similar sets of phages, but lacked certain virulence genes.

Conclusions: Host exchange and regional transmission of ST9 have occurred between pigs and humans. Pig rearing and trading might have favoured gene exchanges between ST9 isolates. Resistance genes, obtained from the environment and other isolates, were stably integrated into the chromosomal DNA. The abundance of resistance genes among ST9 is likely attributed to the extensive use of antimicrobial agents in livestock. Phages are present in the genomes of ST9 and may play a role in the rapid evolution of this ST. Although human ST9 infections are rare, ST9 isolates may constitute a potential risk to public health as a repository of antimicrobial resistance genes.

Introduction

Staphylococcus aureus is a major opportunistic pathogen with a propensity to rapidly develop antimicrobial resistance.[1] MRSA is recognized as a pathogen of global concern,[2] which can also cause diseases in animals.[3,4] The epidemiological history of MRSA has been reshaped since the first report of livestock-associated MRSA (LA-MRSA) transmission to humans.[5] Thus, LA-MRSA has gradually gained attention as an important zoonotic pathogen. The global prevalence and spread of LA-MRSA differs geographically. Unlike the predominance of ST398 in Europe and North America,[1,5–8] clonal complex (CC) 9 is the major LA-MRSA CC in Asia, including China, Malaysia, and Thailand.[6,9,10] Recently, cases of human MRSA ST9 infections have been reported,[9,11,12] indicating that ST9 isolates also pose a risk to human health. One study also showed that some pig-derived MRSA ST9 isolates shared a close phylogenetic relationship with human clinical isolates, suggesting that human- and pig-derived isolates evolved from a common ancestor or that ST9 isolates had been exchanged between humans and animals in either direction.[9]

Over the last decade, high-resolution WGS analysis has been applied to unravel the dynamic evolution of *S. aureus* lineages, including ST398, ST239, ST22, ST30, ST8, ST80 and USA300.[1,13–19] These studies have included a large number of community-acquired and hospital-acquired MRSA isolates and provided insight into the evolution, emergence and transmission dynamics of the respective STs. However in this regard, comparatively little is known about ST9, which harbours a large repertoire of mobile

genetic elements (MGEs), including novel staphylococcal cassette chromosome *mec* (SCC*mec*) elements,[20–23] *S. aureus* pathogenicity islands (SaPIs), and antimicrobial resistance gene clusters.[23] A study showed that MGEs make up 15%–20% of the *S. aureus* genome.[24] It is also worth noting that multiresistance gene clusters, containing the aminoglycoside resistance gene *aadE*, the aminocyclitol resistance gene *spw*, the lincosamide resistance gene *lnu*(B), and the pleuromutilin-lincosamide-streptogramin A (PLS_A) resistance gene *lsa*(E), are widely present in ST9 isolates.[21,25]

Using WGS analysis, we aimed at tracking the spread of MRSA ST9 throughout different areas of China and investigated the evolutionary relationships among isolates. We described the phylogeny of ST9 isolates using a data set of 131 genomes collected between 2002 and 2016 from 11 provinces in China, investigated the novel structure and distribution of the *lsa*(E)-carrying multiresistance gene cluster, and genotyped prophages in the genomes of the ST9 isolates. Overall, our results showed that: (i) ST9 has been spreading in China rapidly since 1987; (ii) MGEs have likely been acquired before ST9 emergence; and (iii) antimicrobial multiresistance has stabilized during evolution.

Materials and methods

Bacterial isolates

The data set used in this study comprised 131 ST9 isolates. Among them, 94 MRSA and MSSA isolates collected by our group were selected for sequencing.[21] The sequences of another 24 isolates had been reported in our previous work.[12] Publicly available WGS data for 13 ST9 isolates was retrieved from the NCBI database (https://trace.ncbi.nih.gov/). The data set consisted of 114 healthy pig-derived and 17 human-derived isolates from 11 provinces (Table 1 and Figure S1, available as Supplementary data at *JAC* Online). All six human clinical isolates were from hospitals in Taiwan and the remaining 11 human isolates from healthy pig-farmers in mainland China.[26] Detailed information regarding all isolates included in this study is provided in Table S1.

DNA preparation, WGS, SNPs and core-genome phylogeny

DNA extraction, library construction, and WGS were carried out as previously described.[27] Two of the genomes were sequenced using the PacBio RSII sequencer (Bionova Biotech Co.). Trimmomatic,[28] Kraken,[29] and FastQC (https://www.bioinformatics.babraham.ac.uk/projects/fastqc) were used for reads quality control. Isolates with low quality reads were excluded from analyses.

Paired-end reads and assemblies ($n = 119$ and $n = 12$, respectively) were mapped against the reference genome of MRSA isolate QD-CD9 (GenBank accession no. NZ_CP031838) using Snippy (https://github.com/tseemann/snippy). The resulting bam files were extracted to filter heterozygous allele calls and generate the core alignment, from which we removed sites and ran Gubbins[30] using default settings to detect homologous recombination events. For each SNP that met the criteria in every isolate, consensus allele calls for SNP loci were extracted from all genomes as described previously.[31] SNPs with confident homozygous allele calls (Phred quality >20) in >90% of the genomes were merged to produce an alignment of 5075 sites.

Maximum likelihood (ML) trees were constructed using RaxML v8.1.23[32] with a general time-reversable (GTR) model and gamma distribution of rate heterogeneity and were performed five times with 100 bootstrap replicates for each run. We selected the tree with the highest likelihood score. We constructed an additional tree that included seven outgroup genomes in the same way without Gubbins running to assure the topology was correct (Figure S2).

Table 1. Numbers of *S. aureus* ST9 isolates from pigs and humans

ST9 isolates	Healthy pig origin	Human (pig farmer) origin		All
		Healthy	Clinical	
MRSA	108	6 (6)	6 (2)	120
MSSA	6	5 (5)	0 (0)	11
All	114	11 (11)	6 (2)	131

Assembly, annotation and pangenome analysis

Unicycler v0.4.4-Beta[33] was used to generate SPAdes v3.10.0 assemblies for the sequences on the Illumina platform and PacBio.[34] Assembled reads were corrected and trimmed using Circlator.[35] Prokka v1.14.5[36] was used to annotate each assembly, while Roary v3.6.0[37] was applied for determining core and accessory genes for all annotated genomes using default parameters. Core genes were defined as those present in at least 95% of genomes.

Detection of resistance/virulence genes and phages

Antimicrobial resistance genes were detected using SRST2 against the ARGannot database,[38] with a cutoff of 90% coverage. The resulting sequences were subjected to BLAST analysis against the NCBI nucleotide database to determine the similarity to previously published sequences. Virulence factors were identified using the VFDB[39] with an 80% identity cutoff. All genomes were screened using PHASTER[40] to detect prophages.

Bayesian molecular clock analysis

The temporal signal was investigated in Tempest v1.5.3.[41] We subsequently used BEAST v2.4.7[42] to estimate a Bayesian phylogeny with divergence dates using a GTR substitution model. In informal model testing, as the coefficient of rate variation parameter was calculated to be 0.91 [95% Highest Posterior Density (HPD) = 0.81–1.01] and the distribution was not abutting zero, a relaxed clock model was favoured over a strict clock model. Notably, the phylogeny generated from this initial analysis showed a different topology from that obtained from the outgroup rooted ML tree, with low posterior probabilities for the deeper nodes, since the maximum clade credibility (MCC) tree topology was erroneously driven. To overcome this problem, we fixed the tree topology to that of the outgroup-rooted and well supported ML tree. BEAST was run with a Markov chain Monte Carlo length of 3×10^9, sampling every 3×10^5 generations, with the first 10% of the data discarded as burn-in. After comparing the results of different model combinations obtained using clock models (strict, uncorrelated relaxed exponential, uncorrelated relaxed lognormal) and demographic models (coalescent constant and exponential), the relaxed lognormal clock with coalescent exponential population defined as the best fitting model priors was used as it produced higher overall likelihoods (Figure S3a, b). Each model was run three times. Good convergence of chains and effective sample size values (≥200) were inspected using Tracer v1.7.1.[43] We conducted date-randomized tests with 20 replications using BEAST and R package TipDatingBeast (Figure S3c).[44]

Data availability

All genomic data are available at NCBI Bioproject database under accession no. PRJNA487590. Additional prophage genomes are available at Genbank under accession nos. NZ_023500.1 (stauST398-2), NC_009762.3 (tp310-2), and NC_020199.1 (phi7401PVL). Outgroup isolates used in the context phylogeny are available from NCBI under accession nos. SAMEA698264

(ST150), SAMEA698556 (ST88), SAMEA698205 (ST109), SAMEA698249 (ST9), SAMEA698727 (ST101), SAMEA698411 (ST101), and SAMEA698577 (ST97).

Results

Test collection

We analysed WGS data of 120 MRSA and 11 MSSA ST9 isolates from pigs ($n = 114$) and humans ($n = 17$), collected in 11 provinces in China between 2002 and 2016 (Figure S1 and Table S1). Only one isolate harboured a pseudo-SCC*mec* XII element,[20] while all remaining MRSA isolates carried an SCC*mec* XII cassette. Except for the isolates FJ-M6 (*spa* type t4358) and TW-TSAR07 (*spa* type t4132), all other isolates were assigned to *spa* type t899, which is consistent with previous studies.[10,21,23,45,46] From the dataset, a total of 18 182 SNPs were extracted from the non-repetitive core-genome. Comparative analysis showed low nucleotide divergence across core-genomes of ST9, with a median pairwise distance of 133 SNPs (range 10–242), and 0.0047% nucleotide divergence (range 0.000035%–0.0085%).

Population structure of ST9 was divided into two clades

A phylogenetic tree constructed from the core-SNPs showed the separation of the ST9 isolates into two distinct lineages, ST9-A ($n = 122$) and ST9-B ($n = 9$) (Figure 1a), supported by 100% bootstrap support of main nodes. The comparison of pairwise SNP distances within and between ST9-A and ST9-B confirmed the validity and the genetic variation of them (Figure 1b). Pig- and human-derived isolates clustered into both sub-clades, while the eight MSSA isolates and one MRSA isolate representing ST9-B were all from rural Shandong.[12] Despite the observation that the ST9 isolates from different provinces showed variable degrees of differentiation as illustrated by the multiple small branches, they were in general closely related. In most cases, porcine MRSA ST9 isolates from the same province or region clustered together (Figure 1a). However, there were also subclusters that comprised ST9 isolates from different regions, e.g. Guangdong, Henan, and Shandong. The observation that there was no significant difference of pairwise SNP distribution among provinces may be interpreted as evidence of isolate exchange (Figure S4).

ST9 emerged around 1987 and evolved at a rapid rate

We detected a strong temporal signal in the alignment (Figure S3d), sufficient to estimate evolutionary rates and dates for the most recent common ancestor (MRCA). Hence, we estimated the divergence date and evolution rates of the ST9 isolates using BEAST. BEAST analysis suggested an initial divergence of the ST9 population in pig farming in approximately 1987 (Figure 2, 95% HPD = 1976 to 1997), which is about 20 years earlier than when ST9 MRSA was first identified among pigs in China.[45] The combined estimate for the substitution rate within the ST9 population was 2.73×10^{-6} per site per year (95% HPD = 1.97×10^{-6} to 3.46×10^{-6}), equivalent to the accumulation of 7.80 SNPs per genome per year (95% HPD = 5.63 to 9.88). The MRCA for the entire ST9-A and ST9-B were estimated to be 1992 (95% HPD = 1985 to 1998) and 2007 (95% HPD = 2001 to 2012), respectively.

ST9 isolates shared similar and stable multiresistance properties

We noted a similar pattern of antimicrobial resistance within the ST9 lineage. Predicted resistance phenotypes across ST9 isolates were common for β-lactam (99.2%), aminoglycoside (100%), aminocyclitol (99.2%), lincosamide (100%), macrolide (64.9%), tetracycline (99.2%), trimethoprim (100%), florfenicol (93.1%), and fluoroquinolone resistance (100%), with a corresponding resistome composed of acquired and chromosomally carried resistance genes and resistance-mediating mutations (Table S1).

Since specific MGEs caused differences between ST9 and other lineages,[23] we examined the involvement of these genomic drivers in the dissemination of the ST9 isolates. In addition to the SCC*mec* XII element, ST9 isolates contained SaPIbov4 (100%), *lsa*(E)-cluster (100%), the *blaZ*-carrying β-lactam resistance transposon Tn*552* (100%), the *aacA-aphD*-carrying aminoglycoside resistance transposon Tn*4001* (70.2%), and the *fexA*-carrying florfenicol resistance transposon Tn*558* (92.4%). We combined the phylogenetic data and the resistance genotype data to speculate about the timeline of genetic events that accompanied the evolution of ST9 (Figure 2). The *lsa*(E)-cluster, SaPI, and *egc* were present in the MRCA of all isolates, assuming that they were likely acquired prior to 1987. Certain MGEs including SCC*mec* XII, Tn*4001*, Tn*552*, SaPI, and the enterotoxin gene cluster had been acquired before 2002, whereas the earliest Tn*558*-harbouring isolate appeared in 2008. Tn*4001* and Tn*558* were lost from several clusters, but remained prevalent in the ST9 isolates. The ST9 population presumably shared most of these MGEs through vertical inheritance because they were present in the oldest isolate. Thus we hypothesized the MGEs most likely stabilized in the genomes of ST9 isolates.

To further test this hypothesis, we investigated the chromosomal structure of the 29 kb *lsa*(E)-cluster in ST9 (Figure 3a). Compared with previous reports,[25,47–49] *lsa*(E)-clusters in our isolates showed more complex structures. The complete structure of the *lsa*(E)-cluster in the genome of NX-T55 consisted of region A (IS*257-repB-aadD*-IS*257*), region B [classical *lsa*(E)-cluster], and region C [*erm*(C)-IS*257*-Tn*4001*], and contained seven resistance genes [*aacA-aphD, aadE, aadD, erm*(C), *tet*(L), *lsa*(E), *lnu*(B), and *spw*]. The conserved region B was observed in all 131 genomes. Many insertion sequences embedded in the clusters indicated that horizontal transfer events might have played a role in the formation of the variants of the *lsa*(E)-cluster. We observed 7 bp direct repeats (5′-CGGGCCA-3′′) between truncated-*repU* and *aadD* in region A that were identical to those in plasmid pG38,[50] suggesting gene transfer events from the plasmid to the chromosome (Figure 3b).

ST9 harboured similar phage structures and lacked certain virulence genes

The accessory genome can be a major driver of adaptation.[51] Therefore, we performed pan-genomic analysis to identify differences among the acquired gene content of the ST9 isolates (Figure S5). We identified a total of 2273 core genes and 2271 accessory genes, with remarkable conservation of the gene content observed among the ST9 genomes. PHASTER analysis revealed that the number of phage sequences ranged from 0–2 (Table S1). We next examined the distribution of seven phage types based on

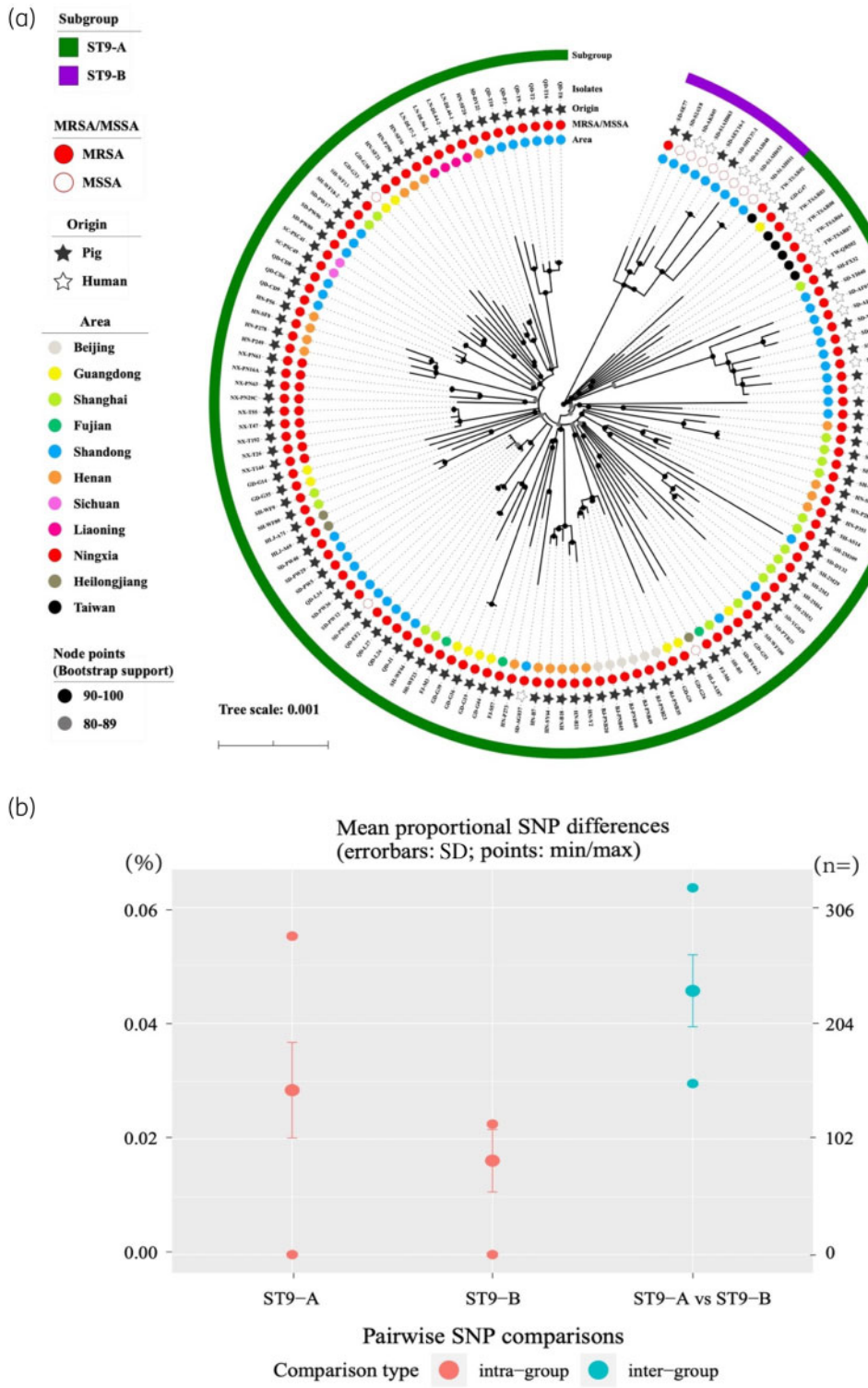

Figure 1. The population structure of ST9. (a) A midpoint-rooted maximum likelihood phylogenetic tree of ST9 ($n = 131$; MRSA = 120, MSSA = 11) based on 18 182 individual SNPs. Black and grey dots on the nodes indicate bootstrap support higher than 90, and from 80 to 90, respectively. Coloured circles in the inner ring and outer ring indicate the different provinces from which the isolates were collected, and the MRSA/MSSA isolates, respectively. The stars represent the sample source. The ST9-A ($n = 122$) and ST9-B ($n = 9$) clades are indicated by green and purple bands. (b) Core-genome pairwise SNP comparisons of within and between ST9-A and ST9-B groups. The groups had smaller within-group diversity than between-group diversity. SD, standard deviation; min, minimum; max, maximum. This figure appears in colour in the online version of *JAC* and in black and white in the print version of *JAC*.

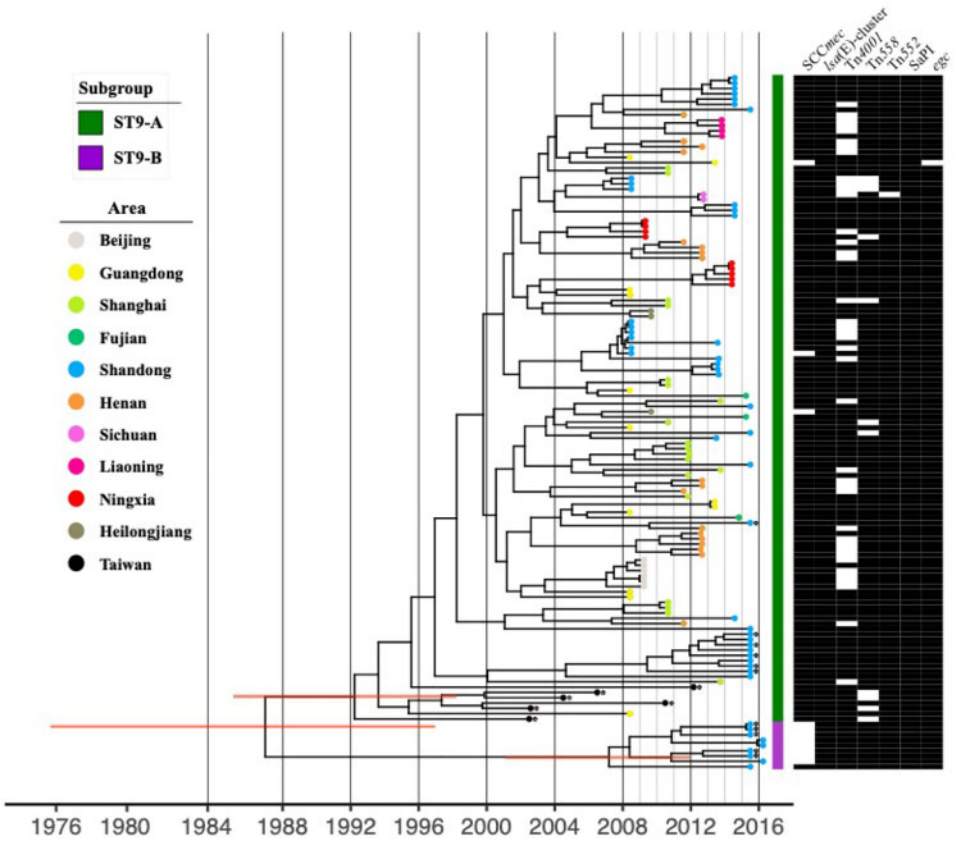

Figure 2. Molecular clock estimate of the emergence of ST9. Shown is the MCC tree for ST9, with the timescale estimated in BEAST using a variable clock model (uncorrelated lognormal). The posterior possibility of each node corresponds to the ML tree. The tips of the tree are constrained by isolation dates. Different MGEs are shown in binary form, where black and white regions represent the presence and absence of the elements, respectively. Tip circles with colours indicate the different areas from which the isolates were collected. The little stars beside the tip points represent human samples. The green and purple binary represents subclade ST9-A and ST9-B, respectively. The red bars indicate the respective 95% highest posterior density intervals of three main differentiation nodes (MRCA, ST9-A, and ST9-B). This figure appears in colour in the online version of *JAC* and in black and white in the print version of *JAC*.

integrase genes.[52,53] Sa2*int* and Sa4*int* were present in 26.0% (34/131) and 33.6% (44/131) of our isolates, while Sa1*int* and Sa5*int* were only found in 3.1% (4/131) and 5.3% (7/131), respectively. Sa2*int* prophages did not carry any known virulence determinants. Sa3*int* prophages were absent from the ST9 lineage despite being present in 90% of *S. aureus* genomes described to date.[54] Thus, ST9 completely lacks some of the staphylococcal enterotoxin and superantigen genes (i.e. *sea*, *sek*, and *tst*), carried on Sa3*int* phages.[55] Genomic structural comparison between the prophages in ST9 isolates revealed a high degree of similarity (Figure S6). We also examined the restriction-modification systems (R-M system) in our isolates. All ST9 isolates harboured an intact type I R-M system which is tightly associated with the lineages or CCs into which *S. aureus* isolates are divided (Table S1).[56]

To further understand the propensity of the ST9 isolates to cause disease, we examined the genome sequences for *S. aureus* virulence factors (Table S1). None of the isolates was positive for genes encoding the Panton–Valentine leucocidin (*lukS/F-PV*). However, all isolates carried genes encoding the α- and β-toxins (*hla* and *hlb*), ɤ-haemolysin (*hlg*A/B/C), and the von Willebrand factor binding protein (*vwb*). Moreover, the ST9 isolates harboured the enterotoxin gene cluster (Table S1), even though the Sa3*int*-encoded *sea* gene was missing.

Discussion

In contrast to the previous research on ST9,[23] our large-scale study provides improved insight into the local evolution and genomic structure of the LA-MRSA ST9 in China. The numbers of samples from each province in our data set is uneven due to the availability of ST9 isolates from the different provinces of China. Other studies have also shown that MRSA ST9 in healthy pigs occurs in the different provinces at various frequencies, estimated to range from 3.6% to 47%, with an average of 11.2%.[10,21] Pig- and human-derived isolates clustered into both sub-clades (ST9-A or ST9-B), suggesting that host exchanges have sometimes occurred between pigs and humans in the evolutionary history of ST9, which has also been demonstrated by other research.[23] Clinical isolates and pig-derived isolates were clustered on the same branch of the phylogenetic tree, suggesting that ST9 has also the ability to colonize humans and might pose a non-negligible threat to the health of both humans and pigs. The observation that isolates from the

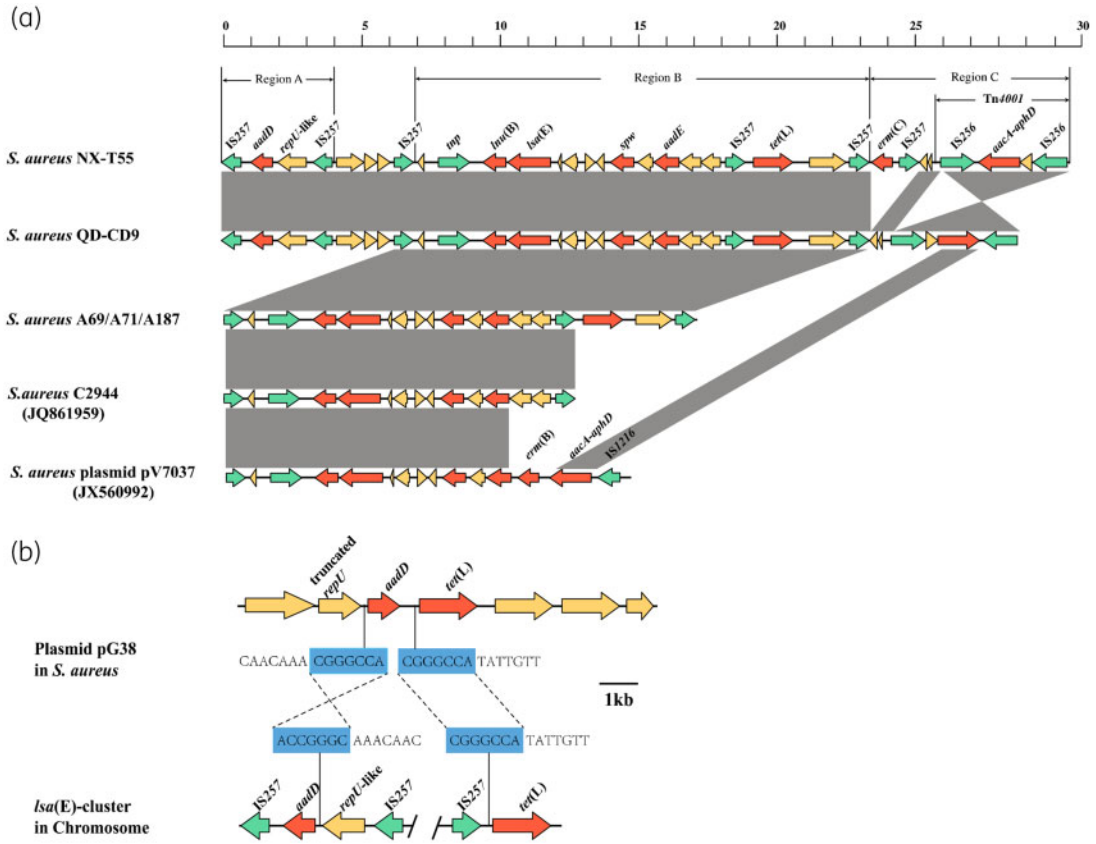

Figure 3. Structural comparison of the *lsa*(E) cluster. (a) Comparative structural analyses of five different types of *lsa*(E)-cluster from five isolates. Isolates NX-T55, QD-CD9, and A69/A71/A187 were included in our data set, while genomic information for isolate C2944 and plasmid pV7037 was retrieved from the NCBI database. Regions of >95% nucleotide sequence identity are indicated by shading. (b) Sequence comparison of plasmid pG38 and parts of the *lsa*(E)-cluster. Open reading frames are shown as arrows, indicating the direction of transcription. Different colours indicate different genes: insertion sequences (green), resistance genes (red), and functional and hypothetical genes (yellow). The 7 bp direct repeats are shown in blue boxes. This figure appears in colour in the online version of *JAC* and in black and white in the print version of *JAC*.

same province clustered together suggested the regional development of ST9, whereas the subclusters comprising isolates from different areas may result from pig trade.

The combination of phylogenetic and molecular clock analyses provided a compelling depiction of the emergence of ST9 from its proposed origins in China around 1987 to its current status as the most prevalent LA-MRSA lineage in China.[10,21,57] The separation of ST9-A and ST9-B indicates the individual evolutionary paths along which the two clades have developed, while the distance between them suggests that their core-genomes are slightly divergent. We did not reconstruct the ancestral state for the reason of the uncertainty in the tree nodes, but according to the molecular clock with binary, we could infer that the main MGEs, such as SCC*mec*, were acquired before the oldest ST9 isolate emerged. The acquisition of SCC*mec* may facilitate the expansion of *S. aureus*,[58] including ST9.

Crucial for the survival of *S. aureus* is the ability to generate genetic point mutations and recombinations, enabling it to rapidly adapt to new ecological niches.[58] A study estimated the rate of recombinations within CCs and concluded that point mutations were at least 15-fold more likely to happen than recombinations.[59] Bayesian analysis suggested that LA-MRSA ST9 has a rapid substitution rate compared with other *S. aureus* STs. The estimated substitution rate of ST9 isolates (2.73×10^{-6}, 95% HPD = 1.97×10^{-6} to 3.46×10^{-6}) was comparatively higher than those reported previously for many *S. aureus* lineages such as ST22 (1.3×10^{-6}, 95% HPD = 1.2×10^{-6} to 1.4×10^{-6}), ST8 (6.15×10^{-7}, 95% HPD = 5.53×10^{-7} to 6.77×10^{-7}), and ST398 (1.49×10^{-6}, 95% HPD = 9.44×10^{-7} to 1.97×10^{-6}), but was similar to that of ST239 (2.2×10^{-6}, 95% HPD = 1.96×10^{-6} to 2.51×10^{-6}).[14,60–62] ST9 emerged in China 20 years later than ST398 in Europe,[63] however, the evolution rate of ST9 was faster, which may be related to the extensive use of antibiotics in the pig industry and the continuous growth of the pig trade at the end of last century. Because of the rapid evolution, more in-depth genomic monitoring of ST9-MRSA in the various regions will be necessary to understand the local epidemiology and evolutionary history. Furthermore, a limitation of the sampling framework used as the basis for this study is that the non-structural sampling and the limited sample size do not provide a sufficiently high confidence level to allow speculation on the geographical spread of the ST9 lineage.

Our data showed that all ST9 isolates have accumulated antimicrobial resistance genes since the early ages of the lineage. As an evolutionary advantage in the presence of selective pressure,

many MGEs are stably present in the ST9 genome. The observed integration of IS*257*-*aadD*-(*repU*-like)-IS*257* and Tn*4001* into the chromosomal *lsa*(E)-cluster, within which genes are more stable than in plasmids, suggested that the integration process was mediated by IS*257* which has been involved in chromosomal integration and plasmid co-integrate formation processes in staphylococci.[64,65] The abundance of MGEs suggests that the success of ST9 isolates in colonization of various hosts is likely the result of a specific mobilome content. *S. aureus* from animals can be a reservoir of antimicrobial resistance genes,[66] and disseminate MGEs to other members of the bacterial population, occasionally by enhancing their pathogenicity.[67] Hence, the wide distribution of ST9 isolates raises the possibility that these isolates are important donors of MGEs to other environmental bacteria.

Phages play an important role in gene transfer and phage-mediated transmission of virulence genes may be affected by the phage type and limitations associated with the lineage of the host bacterium.[68,69] The ST9 isolates do not carry known virulence factors associated with human diseases, and, therefore, are likely to be less virulent. Sa3*int* prophage, which reportedly harbours virulence genes such as *sak, chp* and *scn* that encode modulators of the human innate immune response, appears to be completely absent in the ST9 lineage, suggesting ST9 is more adaptive to animals than humans. Under long-term antimicrobial selection pressure, MGEs may have been exchanged within the ST9 lineage, resulting in similar antimicrobial resistance phenotypes and genotypes. In addition, ST9 phages had a high degree of homology to phage stauST398_2 of the CC398 isolate SO385. It is worth noting that LA-MSSA CC398 is also occasionally detected in China.[21,45,56] Notably, a study has shown that ST9 existed in Europe before the emergence of CC398.[70] In other studies conducted in the United States, ST9 was one of the most common MSSA STs in pigs.[70,71]

The acquisition of multiresistance is considered as one plausible explanation for the successful emergence of ST9 in China.[10,21–23] The prevalence of resistance genes among the ST9 isolates is likely attributed to the extensive use of antimicrobial feed additives in livestock rearing,[72] with the consequence of the rapid evolution. The observed high antimicrobial resistance rates for β-lactams, tetracyclines, florfenicol, and fluoroquinolones among others, reflect the sales and consumption figures of veterinary antimicrobial agents used in pig breeding industry in China.[72] The future will show whether traditional Chinese medicine[73] can replace or reduce the use of antimicrobial agents in pigs and thereby lower the selection pressure.

Funding

This work was funded by the National Natural Science Foundation of China (31761133022 and 81861138051) and the German Research Foundation (SCHW382/11-1).

Transparency declarations

None to declare.

Supplementary data

Table S1 and Figures S1 to S6 are available as Supplementary data at *JAC* Online.

References

1 Price LB, Stegger M, Hasman H *et al*. *Staphylococcus aureus* CC398: host adaptation and emergence of methicillin resistance in livestock. *MBio* 2012; **3**: e00305-11.

2 Pantosti A, Sanchini A, Monaco M. Mechanisms of antibiotic resistance in *Staphylococcus aureus*. *Future Microbiol* 2007; **2**: 323–34.

3 Verkade E, Kluytmans J. Livestock-associated *Staphylococcus aureus* CC398: animal reservoirs and human infections. *Infect Genet Evol* 2014; **21**: 523–30.

4 Cuny C, Friedrich A, Kozytska S *et al*. Emergence of methicillin-resistant *Staphylococcus aureus* (MRSA) in different animal species. *Int J Med Microbiol* 2010; **300**: 109–17.

5 Voss A, Loeffen F, Bakker J *et al*. Methicillin-resistant *Staphylococcus aureus* in pig farming. *Emerg Infect Dis* 2005; **11**: 1965–6.

6 Chuang YY, Huang YC. Livestock-associated meticillin-resistant *Staphylococcus aureus* in Asia: an emerging issue? *Int J Antimicrob Agents* 2015; **45**: 334–40.

7 Smith TC, Pearson N. The emergence of *Staphylococcus aureus* ST398. *Vector Borne Zoonotic Dis* 2011; **11**: 327–39.

8 Chairat S, Gharsa H, Lozano C *et al*. Characterization of *Staphylococcus aureus* from raw meat samples in Tunisia: detection of clonal lineage ST398 from the African Continent. *Foodborne Pathog Dis* 2015; **12**: 686–92.

9 Wan MT, Lauderdale TL, Chou CC. Characteristics and virulence factors of livestock associated ST9 methicillin-resistant *Staphylococcus aureus* with a novel recombinant staphylocoagulase type. *Vet Microbiol* 2013; **162**: 779–84.

10 Cui S, Li J, Hu C *et al*. Isolation and characterization of methicillin-resistant *Staphylococcus aureus* from swine and workers in China. *J Antimicrob Chemother* 2009; **64**: 680–3.

11 Liu Y, Wang H, Du N *et al*. Molecular evidence for spread of two major methicillin-resistant *Staphylococcus aureus* clones with a unique geographic distribution in Chinese hospitals. *Antimicrob Agents Chemother* 2009; **53**: 512–8.

12 Sun C, Chen B, Hulth A *et al*. Genomic analysis of *Staphylococcus aureus* along a pork production chain and in the community, Shandong Province, China. *Int J Antimicrob Agents* 2019; **54**: 8–15.

13 Harris SR, Feil EJ, Holden MT *et al*. Evolution of MRSA during hospital transmission and intercontinental spread. *Science* 2010; **327**: 469–74.

14 Holden MT, Hsu LY, Kurt K *et al*. A genomic portrait of the emergence, evolution, and global spread of a methicillin-resistant *Staphylococcus aureus* pandemic. *Genome Res* 2013; **23**: 653–64.

15 McAdam PR, Templeton KE, Edwards GF *et al*. Molecular tracing of the emergence, adaptation, and transmission of hospital-associated methicillin-resistant *Staphylococcus aureus*. *Proc Natl Acad Sci USA* 2012; **109**: 9107–12.

16 Uhlemann AC, Dordel J, Knox JR *et al*. Molecular tracing of the emergence, diversification, and transmission of *S. aureus* sequence type 8 in a New York community. *Proc Natl Acad Sci USA* 2014; **111**: 6738–43.

17 Stegger M, Wirth T, Andersen PS *et al*. Origin and evolution of European community-acquired methicillin-resistant *Staphylococcus aureus*. *MBio* 2014; **5**: e01044-14.

18 DeLeo FR, Kennedy AD, Chen L *et al*. Molecular differentiation of historic phage-type 80/81 and contemporary epidemic *Staphylococcus aureus*. *Proc Natl Acad Sci USA* 2011; **108**: 18091–6.

19 Larsen J, Stegger M, Andersen PS *et al*. Evidence for human adaptation and foodborne transmission of livestock-associated methicillin-resistant *Staphylococcus aureus*. *Clin Infect Dis* 2016; **63**: 1349–52.

20 Jiang N, Li J, Feßler AT *et al*. Novel pseudo-staphylococcal cassette chromosome *mec* element (phiSCC*mec*$_{T55}$) in MRSA ST9. *J Antimicrob Chemother* 2019; **74**: 819–20.

21 Li J, Jiang N, Ke Y *et al.* Characterization of pig-associated methicillin-resistant *Staphylococcus aureus*. *Vet Microbiol* 2017; **201**: 183–7.

22 Bi Z, Sun C, Borjesson S *et al.* Identical genotypes of community-associated MRSA (ST59) and livestock-associated MRSA (ST9) in humans and pigs in rural China. *Zoonoses Public Health* 2018; **65**: 367–71.

23 Zhou W, Li X, Osmundson T *et al.* WGS analysis of ST9-MRSA-XII isolates from live pigs in China provides insights into transmission among porcine, human and bovine hosts. *J Antimicrob Chemother* 2018; **73**: 2652–61.

24 Lindsay JA. Genomic variation and evolution of *Staphylococcus aureus*. *Int J Med Microbiol* 2010; **300**: 98–103.

25 Li B, Wendlandt S, Yao J *et al.* Detection and new genetic environment of the pleuromutilin-lincosamide-streptogramin A resistance gene *lsa*(E) in methicillin-resistant *Staphylococcus aureus* of swine origin. *J Antimicrob Chemother* 2013; **68**: 1251–5.

26 Chen CJ, Lauderdale TY, Lu CT *et al.* Clinical and molecular features of MDR livestock-associated MRSA ST9 with staphylococcal cassette chromosome *mec*XII in humans. *J Antimicrob Chemother* 2018; **73**: 33–40.

27 Sun C, Zhang P, Ji X *et al.* Presence and molecular characteristics of oxazolidinone resistance in staphylococci from household animals in rural China. *J Antimicrob Chemother* 2018; **73**: 1194–200.

28 Bolger AM, Lohse M, Usadel B. Trimmomatic: a flexible trimmer for Illumina sequence data. *Bioinformatics* 2014; **30**: 2114–20.

29 Wood DE, Salzberg SL. Kraken: ultrafast metagenomic sequence classification using exact alignments. *Genome Biol* 2014; **15**: R46.

30 Croucher NJ, Page AJ, Connor TR *et al.* Rapid phylogenetic analysis of large samples of recombinant bacterial whole genome sequences using Gubbins. *Nucleic Acids Res* 2015; **43**: e15.

31 Perrin A, Larsonneur E, Nicholson AC *et al.* Evolutionary dynamics and genomic features of the *Elizabethkingia anophelis* 2015 to 2016 Wisconsin outbreak strain. *Nat Commun* 2017; **8**: 15483.

32 Stamatakis A. RAxML version 8: a tool for phylogenetic analysis and post-analysis of large phylogenies. *Bioinformatics* 2014; **30**: 1312–3.

33 Wick RR, Judd LM, Gorrie CL *et al.* Unicycler: resolving bacterial genome assemblies from short and long sequencing reads. *PLoS Comput Biol* 2017; **13**: e1005595.

34 Bankevich A, Nurk S, Antipov D *et al.* SPAdes: a new genome assembly algorithm and its applications to single-cell sequencing. *J Comput Biol* 2012; **19**: 455–77.

35 Hunt M, De Silva N, Otto TD *et al.* Circlator: automated circularization of genome assemblies using long sequencing reads. *Genome Biol* 2015; **16**: 294.

36 Seemann T. Prokka: rapid prokaryotic genome annotation. *Bioinformatics* 2014; **30**: 2068–9.

37 Page AJ, Cummins CA, Hunt M *et al.* Roary: rapid large-scale prokaryote pan genome analysis. *Bioinformatics* 2015; **31**: 3691–3.

38 Inouye M, Dashnow H, Raven LA *et al.* SRST2: rapid genomic surveillance for public health and hospital microbiology labs. *Genome Med* 2014; **6**: 90.

39 Chen L, Zheng D, Liu B *et al.* VFDB 2016: hierarchical and refined dataset for big data analysis—10 years on. *Nucleic Acids Res* 2016; **44**: D694–7.

40 Arndt D, Grant JR, Marcu A *et al.* PHASTER: a better, faster version of the PHAST phage search tool. *Nucleic Acids Res* 2016; **44**: W16–21.

41 Rambaut A, Lam TT, Max Carvalho L *et al.* Exploring the temporal structure of heterochronous sequences using TempEst (formerly Path-O-Gen). *Virus Evol* 2016; **2**: vew007.

42 Bouckaert R, Heled J, Kuhnert D *et al.* BEAST 2: a software platform for Bayesian evolutionary analysis. *PLoS Comput Biol* 2014; **10**: e1003537.

43 Rambaut A, Drummond AJ, Xie D *et al.* Posterior summarization in Bayesian phylogenetics using Tracer 1.7. *Syst Biol* 2018; **67**: 901–4.

44 Rieux A, Khatchikian CE. TIPDATINGBEAST: an R package to assist the implementation of phylogenetic tip-dating tests using beast. *Mol Ecol Resour* 2017; **17**: 608–13.

45 Wagenaar JA, Yue H, Pritchard J *et al.* Unexpected sequence types in livestock associated methicillin-resistant *Staphylococcus aureus* (MRSA): MRSA ST9 and a single locus variant of ST9 in pig farming in China. *Vet Microbiol* 2009; **139**: 405–9.

46 Fang HW, Chiang PH, Huang YC. Livestock-associated methicillin-resistant *Staphylococcus aureus* ST9 in pigs and related personnel in Taiwan. *PLoS One* 2014; **9**: e88826.

47 Lozano C, Aspiroz C, Saenz Y *et al.* Genetic environment and location of the *lnu*(A) and *lnu*(B) genes in methicillin-resistant *Staphylococcus aureus* and other staphylococci of animal and human origin. *J Antimicrob Chemother* 2012; **67**: 2804–8.

48 Li XS, Dong WC, Wang XM *et al.* Presence and genetic environment of pleuromutilin-lincosamide-streptogramin A resistance gene *lsa*(E) in enterococci of human and swine origin. *J Antimicrob Chemother* 2014; **69**: 1424–6.

49 Wendlandt S, Feßler AT, Monecke S *et al.* The diversity of antimicrobial resistance genes among staphylococci of animal origin. *Int J Med Microbiol* 2013; **303**: 338–49.

50 Jiang N, Li J, Feßler AT *et al.* A novel small *tet*(T)-*tet*(L)-*aadD*-carrying plasmid from MRSA and MSSA ST9 isolates of swine origin. *J Antimicrob Chemother* 2019; **74**: 2462–4.

51 Lindsay JA, Holden MTG. *Staphylococcus aureus*: superbug, super genome? *Trends Microbiol* 2004; **12**: 378–85.

52 Kahankova J, Pantucek R, Goerke C *et al.* Multilocus PCR typing strategy for differentiation of *Staphylococcus aureus* siphoviruses reflecting their modular genome structure. *Environ Microbiol* 2010; **12**: 2527–38.

53 Deghorain M, Van Melderen L. The staphylococci phages family: an overview. *Viruses* 2012; **4**: 3316–35.

54 Goerke C, Wirtz C, Fluckiger U *et al.* Extensive phage dynamics in *Staphylococcus aureus* contributes to adaptation to the human host during infection. *Mol Microbiol* 2006; **61**: 1673–85.

55 Holtfreter S, Grumann D, Schmudde M *et al.* Clonal distribution of superantigen genes in clinical *Staphylococcus aureus* isolates. *J Clin Microbiol* 2007; **45**: 2669–80.

56 Waldron DE, Lindsay JA. Sau1: a novel lineage-specific type I restriction-modification system that blocks horizontal gene transfer into *Staphylococcus aureus* and between *S. aureus* isolates of different lineages. *J Bacteriol* 2006; **188**: 5578–85.

57 Li W, Liu JH, Zhang XF *et al.* Emergence of methicillin-resistant *Staphylococcus aureus* ST398 in pigs in China. *Int J Antimicrob Agents* 2018; **51**: 275–6.

58 Narra HP, Ochman H. Of what use is sex to bacteria? *Curr Biol* 2006; **16**: R705–10.

59 Feil EJ, Cooper JE, Grundmann H *et al.* How clonal is *Staphylococcus aureus*? *J Bacteriol* 2003; **185**: 3307–16.

60 Uhlemann AC, McAdam PR, Sullivan SB *et al.* Evolutionary dynamics of pandemic methicillin-sensitive *Staphylococcus aureus* ST398 and its international spread via routes of human migration. *MBio* 2017; **8**: e01375-16.

61 Hsu LY, Harris SR, Chlebowicz MA *et al.* Evolutionary dynamics of methicillin-resistant *Staphylococcus aureus* within a healthcare system. *Genome Biol* 2015; **16**: 81.

62 Challagundla L, Luo X, Tickler IA *et al.* Range expansion and the origin of USA300 north American epidemic methicillin-resistant *Staphylococcus aureus*. *MBio* 2018; **9**: e02016-17.

63 Devriese LA, Vandamme LR, Fameree L. Methicillin (Cloxacillin)-resistant *Staphylococcus aureus* strains isolated from bovine mastitis cases. *Zentralbl Veterinarmed B* 1972; **19**: 598–605.

64 Hesselbarth J, Werckenthin C, Liebisch B *et al*. Insertion elements in *Staphylococcus intermedius*. *Lett Appl Microbiol* 1995; **20**: 180–3.

65 Schwarz S, Feßler AT, Hauschild T *et al*. Plasmid-mediated resistance to protein biosynthesis inhibitors in staphylococci. *Ann N Y Acad Sci* 2011; **1241**: 82–103.

66 Argudin MA, Deplano A, Meghraoui A *et al*. Bacteria from animals as a pool of antimicrobial resistance genes. *Antibiotics (Basel)* 2017; **6**: 12.

67 Bruen TC, Philippe H, Bryant D. A simple and robust statistical test for detecting the presence of recombination. *Genetics* 2006; **172**: 2665–81.

68 Goerke C, Pantucek R, Holtfreter S *et al*. Diversity of prophages in dominant *Staphylococcus aureus* clonal lineages. *J Bacteriol* 2009; **191**: 3462–8.

69 McCarthy AJ, Witney AA, Lindsay JA. *Staphylococcus aureus* temperate bacteriophage: carriage and horizontal gene transfer is lineage associated. *Front Cell Infect Microbiol* 2012; **2**: 6.

70 Espinosa-Gongora C, Moodley A, Lipinska U *et al*. Phenotypes and genotypes of old and contemporary porcine strains indicate a temporal change in the *S. aureus* population structure in pigs. *PLoS One* 2014; **9**: e101988.

71 Linhares LL, Yang M, Sreevatsan S *et al*. The effect of anatomic site and age on detection of *Staphylococcus aureus* in pigs. *J Vet Diagn Invest* 2015; **27**: 55–60.

72 Kirchhelle C. Pharming animals: a global history of antibiotics in food production (1935–2017). *Palgrave Commun* 2018; **4**: 96.

73 Su T, Qiu Y, Hua X *et al*. Novel opportunity to reverse antibiotic resistance: to explore traditional Chinese medicine with potential activity against antibiotics-resistance bacteria. *Front Microbiol* 2020; **11**: 610070.